Article:

Xu, Q, Shen, J, Ran, X et al. (3 more authors) (2021) Robust Transcoding Sensory Information With Neural Spikes. IEEE Transactions on Neural Networks and Learning Systems. pp. 1-12. ISSN 2162-237X

https://doi.org/10.1109/tnnls.2021.3107449

Robust transcoding sensory information with neural spikes

Qi Xu, Jiangrong Shen, Xuming Ran, Huajin Tang, Gang Pan and Jian K. Liu

***Abstract*—Neural coding, including encoding and decoding, is one of the key problems in neuroscience for understanding how the brain uses neural signals to relate sensory perception and motor behaviors with neural systems. However, most of the existed studies only aim at dealing with the analogy signal of neural systems, while lacking a unique feature of biological neurons, termed spike, which is the fundamental information unit for neural computation as well as a building block for brain-machine interface. Aiming at these limitations, we propose a transcoding framework to encode multi-modal sensory information into neural spikes, then reconstruct stimuli from spikes. Sensory information can be compressed into 10% in terms of neural spikes, yet re-extract 100% of information by reconstruction. Our framework can not only feasibly and accurately reconstruct dynamical visual and auditory scenes, but also rebuild the stimulus patterns from functional magnetic resonance imaging brain activities. Importantly, it has a superb ability of noise-immunity for various types of artificial noises and background signals. The proposed framework provides efficient ways to perform multimodal feature representation and reconstruction in a high-throughput fashion, with potential usage for efficient neuromorphic computing in a noisy environment.**

***Index Terms*—Neural Spikes, Cross-Multimodal, Reconstruction, Decoding, Spatio-temporal Representations, Denoising.**

I. INTRODUCTION

SENSORY information is an essential and integrative part of the brain for processing the environment we are in [1]. The most basic stage of sensory perception is to recall the information perceived for higher cognition. Thus, intelligence machines are demanding an ability of representation and reconstruction of sensory information captured by various sensors, to achieve remarkably good computational intelligence tasks. Although various engineering effort has been made in this area, the biological information processing system still outperforms the best artificial systems in many fields such as processing cross-modalities and noise-immunity.

Qi Xu is with School of Artificial Intelligence, Faculty of Electronic Information and Electrical Engineering, Dalian University of Technology, Dalian, 116024, China. (xuqi@dlut.edu.cn)

Qi Xu, Jiangrong Shen, Huajin Tang and Gang Pan are with the College of Computer Science and Technology, Zhejiang University, Zhejiang, 310027, China. (xuqi123@zju.edu.cn, jrshen@zju.edu.cn, htang@zju.edu.cn, gpan@zju.edu.cn)

Qi Xu, Jiangrong Shen and Jian K. Liu are with the Centre for Systems Neuroscience, Department of Neuroscience, Psychology and Behaviour, University of Leicester, Leicester, LE1 7RH, UK.

Jiangrong Shen is also with Qiushi Academy for Advanced Studies, Zhejiang University, Hangzhou, 310027, China and Gang Pan is also with the State Key Lab of CAD & CG, Zhejiang University, Hangzhou 310027, China.

Xuming Ran is with the Department of Biomedical Engineering, Southern University of Science and Technology, Shenzhen, 518055, China.

Jian K. Liu is also with the School of Computing, University of Leeds, Leeds, LS2 9JT, UK. (j.liu9@leeds.ac.uk)

Currently, our brain brings various types of sensor information with different sensory modalities from our surrounding environment. For which, neural coding is very essential for comprehending how neural systems respond to outside stimuli [2]. From the functional part of view, an efficient and effective coding system consists of two elementary parts, neural encoding and decoding [3] [4]. Encoding methods try to transfer outside stimuli into specific responses for further processing by downstream neural systems, then decoding aims to analyse and predict external stimuli from those specific format of data encoded by the encoding system. In biological coding system, neurons transmit the information when they receive the external stimuli by changing their membrane potential to fire a series of fast event termed spikes, forming spatio-temporal representations [5]. Thus spikes have been suggested as a more biological format to represent the input-output relations in neural systems than any other artificial one [6] [7], such as choosing real value based data as transmission media in artificial neural networks [8].

For encoding and decoding in biological information processing systems, there still remain big challenges to understanding the mapping between those external stimuli and fundamental spiking activities. For decoding, although some traditional methods have made significant progresses [9] [10], most of them tried to build artificial models with simple linear models and the questions are limited to either brain activity pattern classification or visual stimuli recognition measured by functional magnetic resonance imaging (fMRI) [11] [12]. On the other hand, deep learning models have enjoyed a great success in many areas of computer vision [8], it is very common for modern artificial deep neural networks (DNNs) to have tens of millions of parameters which lead to higher dimensional complexity and hierarchical structures. Inspired by biologically visual systems, hierarchical DNNs, using convolutional and pooling units to code external stimuli, have already shown in resembling some complex visual representations in human visual system [13]. For visual scenes, convolutional neural networks (CNNs) have been adopted to model the encoding of visual neurons, such as from retina, visual cortex to inferotemporal cortex [14] [15]. Thus, it is promising to build a more reasonable coding system between external stimuli and neural information processing with the aid of spiking activities and the structures of DNNs [7] [16]. Recent studies show that it is promising to use DNNs working with neural spikes for both encoding and decoding [17], [18], [2].

Inspired by the aforementioned studies, this paper proposes an efficient and effective coding system with neural spikes for sensory information based on deep learning network models, named as deep spike pattern decoder (DSPD), that universally transcodes sensory information across multiple sensory modalities using neural spikes. Based on our recent work on decoding with neural spikes [18], the DSPD is an uniform coding framework consists of two parts: encoding and decoding. The encoding part maps outside sensory stimuli into image pixels, than transcodes pixels into neural representations efficiently in two ways. First in the spatial domain, compared to the high dimension of thousands of pixels, it only use a few hundreds of neurons to represented 100% of image pixels into 10% of neural spikes. Secondly, in the time domain, it can sample high-frequency images in videos into a spare temporal patterns, e.g., 30-60 Hz frame rates down to a few Hzs neural spikes firing sparsely over time. The transcoded spatialtemporal patterns in terms of neural spikes can be outputted and transferred in a high-throughput fashion to any downstream hardware for future processing.

Based on transcoded spiking representations, one can conduct any types of neural computation for practical tasks, ranging from classification, semantic recognition, to full-frame reconstruction. Here we show the capacity of our proposed framework in the context of coding of cross-multimodal sensory information, and its good capability of transfer learning, few-shot learning, and stimulus denoising. We evaluated our model on three different types of modal inputs: images, fMRI brain activities, and sound signals. In order to show the generalization ability, we applied the model to the clean and noise-free MNIST dataset and its four variations with strong noises and unrelated background signals. We also take the subsets from these datasets to show the capability of our model on few-shot learning. Experimental results demonstrate that our model is not only capable of perceiving and reconstructing corss-multimodal inputs (images, fMRI and sounds), but also having a good ability of generalization and noise-immunity. The qualitative and quantitative measurements show that our model can construct multimodal stimuli with a performance comparable to some other cognitive models. All together, our model provides an uniform and consistent coding system for efficiently and effectively transcodng sensory information via neural spikes. Inspired by biological underpinnings of how cross-multimodal patterns are perceived and represented by neural processing systems, our work suggest an approach of neuromorphic computing with neural spikes for handling multiple sources of sensor information.

II. Methods

The proposed DSPD is a framework with a mixture of a biological encoding part and a deep neural nwtwork (DNN) based decoding part as illustrated in Figure 1. The encoding part is similar to an neural pathway of the sensory systems, which receive sensory information in the format of images, sound waves, or other types of artificial sensor data represented spatial, temporal, or spatiotemporal patterns. The output of the encoder is a sequence of spikes similar to biological neurons in response to stimuli. After encoding, the encoded information will be delivered to the decoding part. Depending on practical tasks, the different decoders can be built for signal reconstruction, object recognition, semantic classification, etc. One can decode the spikes directly with spiking neural networks as decoder. Or one can also convert spikes into different format of data, for example, image pixels, to take advantage of the state-of-the-art computer vision techniques. The benefit of transcoding sensory information with neural spikes is to utilize the core concept of neuromorphic computing, e.g., energy and data efficient computing without loss of any information. Thus, our proposed framework is a unified spike transcoding system functioning as data compression, feature extraction, temporal encoding and decoding.

In this study, we put our proposed framework into the context of signal reconstruction in terms of image pixels. However, it is noted that our framework is fixable to account for other purposes, so that the exact architectures of the encoder and decoder are fixable to adapt to be other types of neural networks, or simple traditional statistical methods.

A. Transcoding with spikes

A spiking based encoding method differs from which in conventional DNNs. For a pattern recognition such as image classification task, DNNs usually take the raw pixel based value as input directly. In contrast, the spiking based encoding method would map those pixels into binary spike events that happen over time. Depending on data format, one can preprocess the raw sensory information by converting them into image pixels, for example, transferring sound waveforms into spectrograms of image pixels. Here the input images were unified as a size of 64×64. Then an encoder is applied to images to convert them into spikes.

Unlike the previous study [18] where the encoder consists of a small number of retinal neurons. Here we used a set of 300 neurons to cover the whole image space. It is noted that with larger sizes of input images, one can use more number of neurons for encoding. All the encoding neurons were sampled over the entire image space, such that each neuron is located at a specific position in image space. The nonlinear filters are based on the receptive fields of 80 RGCs measured in experiment with white noise analysis [19] fitted with a 2D Gaussian for each cell. We then resampled the receptive fields of all 300 cells by rotating and shifting those experimental 80 cells to cover the pixel space of images, in this way one can overcome the underrepresented location bias due to the limitation of experimental recordings [20]. In addition, we used three subunits for each encoding neuron to utilize the idea of nonlinear subunits of sensory neurons. Each subunit has a Gaussian filter as the receptive field to capture a local image patch. Then the filtered image generates a value of mean over all pixels, which is transferred to obtain a spike count. Binary spikes are sampled from this processing to obtain a spatiotemporal spike pattern. We also tested other filters to generate spikes from inputs. Parameters of encoding neurons are not sensitive to the model outputs, as the spike pattern from the encoding neurons is playing a role of low-dimension representing of inputs, which is not participated into the training of the decoding part.

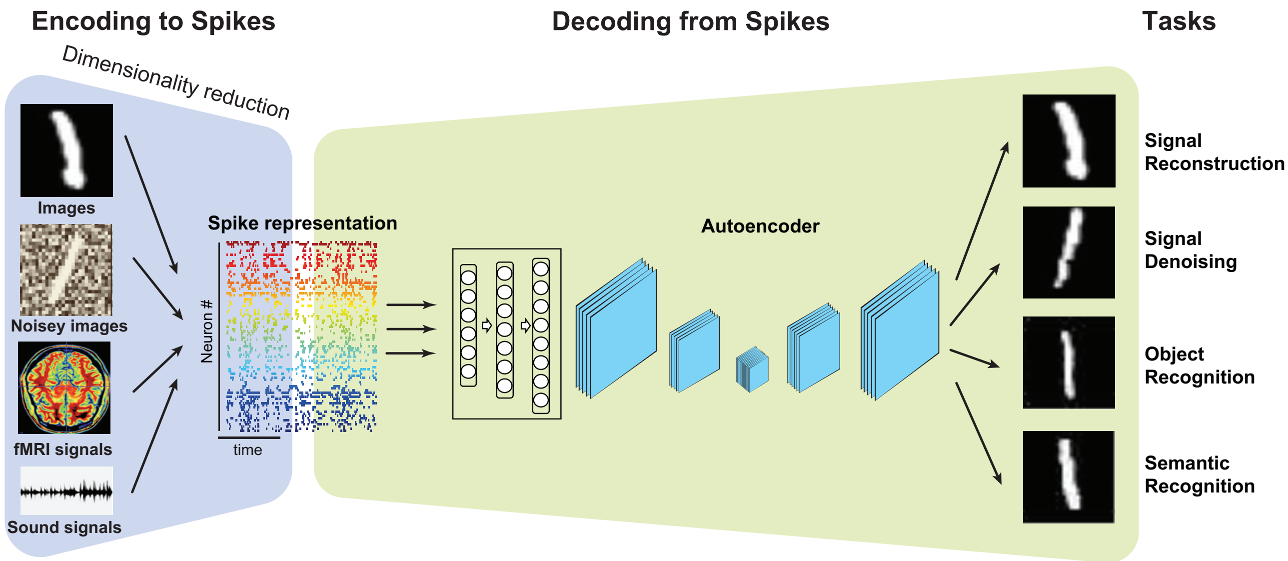

Fig. 1: The schematic diagram of DSPD framework.

B. Pattern decoding with spikes

After encoding, sensory information is represented by a sequence of spatiotemporal spiking pattern. To fulfill our aim of signal reconstruction, we used a similar decoder as in our recent work [18]. We first upsampled the spatial dimension into the original input image size. Then we used a three-layer fully-connected neural network, which is similar to a multilayer perceptron. The first layer receives the spikes coming from the neural encoding layer and the number of the neurons in the first layer is the same as the neurons of neural encoding layer. here 300, e.g., the same dimension as the number of neuorns used for spiking representation. With the 512 neurons in second layer (hidden layer) and 4096 neurons in third layer (output layer), we used the ReLU as activation functions to filter the non-negative value into image pixels. As input images are 64×64, 4096 neurons were used in third layer as the output for signal reconstruction.

The propose of this upsampled image from spikes is to reconstruct the original signals, such that both have the same dimension. In case of implementing other tasks, upsampled images are not necessary. For the signal reconstruction, we adopt a typical autoencoder based on convolutional neural networks. This autoencoder consists of two parts as shown in Figure 1. In the first phase, the convolutional parts down sample the spike-based images. Notably, the most important part of the spike-based images are kept for recovering the texture and increasing the size. Meanwhile, through the decreasing size of convolutional units, the noise and redundant components are filtered. Then the filtered images will recover through the increasing size of convolutional units in the up-sampling phase.

The size of the autoencoder here we used is 64C7-128C5-256C3-256C3-US2-256C3-US2-128C3-US2-64C5-US2 (C means convolutional layer, US means upsampling). The activation function is ReLU and the dropout rate is 0.25, we also use strides (2, 2) for padding and batch normalization for accelerating the training to achieve the convergence state respectively.

Given an input pattern X, it will trigger a response $\mathbf{s} = \{s_1, s_2, s_3 ... s_n\}$ within the encode method we just described on the 300 RGCs, here we adopt spike firing rate such as s_i in $\mathbf{s}$ to represent the spike count of each RGC cell within a bin based on the sampling rating of pattern. Then the triggered responses are first fed into spike-image dense layer based converter which output an intermediate image $Y_1 = f_1(X)$, then the image-image autoencoder takes the $Y1$ as input to map it to match the target pattern. So we can get a refining reconstruction pattern $Y_2 = f_2(Y_1)$, and the end-end training could be implemented by the two joint parts. f_1 and f_2 are their corresponding activation function, in this paper we adopted ReLU. Based on this information flow, we could get the training loss function, $loss = \lambda_1 \|Y_1 - X\| + \lambda_2 \|Y_2 - X\|$. With this loss function, the proposed model could be trained successfully.

C. Datasets and codes

As shown in Figure 1, we evaluate our model on three different types of signals (visual images, fMRI brain activity patterns, and sound signals [21] [22]). Specifically, we employed various different datasets: orginal MNIST with 10 digital letters [23], MNIST with random white noise [24], MNIST with background images [24], MNIST with different level of artificial noise. fMRI brain activity datasets [25] Fig. 5) and sound signals of 10 spoken letter datasets [26].

We used a dataset of fMRI brain activity using handwritten letter images as stimuli [25], which is fMRI imaging of humans containing 360 gray-scale handwritten character images. It has equal number of character B, R, A, I, N, S. The original image resolution is 56 × 56 and the corresponding fMRI signals contain voxels (each fMRI character pattern has 2420 voxels) from V1 and V2 areas of all three subjects S1, S2 and S3.

We also test our model on sound signals. We choose 0-9 digits of T1-46 speech corpus [27] with the audio samples read by 16 speakers for the 10 digits as in MNIST with 4136 audio samples totally. This sound-image dataset is divided into 4000 for training and 136 for testing. During the training process, the pairs of audio-image are used as the training samples simultaneously which are the same digital samples in noise image-image datasets and fMRI-image datasets. We used Auditory toolbox [28] for pre-processing the data, such that all of the audio samples are converted as the spectrograms with 1500 time steps and 39 frequencies, then we can get the a 58,500 × 1 vector (1500 × 39) for each sample.

Although these signals have different dimensionality, we adjusted their sizes and the number of encoding neurons according to the computational ability of the machine. In our cases, the experiments were conducted on a workstation equipped with two-processor Intel(R) Xeon(R) Core CPU and one NVidia GeForce GTX 2080Ti GPU. The operating system is Ubuntu 16.04. Tensorflow [29] and Keras [30] were used for implementing our model.

D. Performance evaluation

We choose three different evaluating metrics to evaluate the performance on the proposed DSPD and other compared methods.

1) Mean Square Error (MSE): MSE represents the final expectation of the squared error between the desired and original values. A detailed description of the MSE about the pair of patterns $\langle \mathbf{X}_1, \mathbf{X}_2 \rangle$, with the resolution of $H \times W$ is as follow:

$$MSE = \frac{1}{H \times W} \sum_{i=1}^{H} \sum_{j=1}^{W} ((\mathbf{X}_1(i,j) - \mathbf{X}_2(i,j))^2, \quad (1)$$

Generally, lower MSE value means better pattern quality.

2) Structural Similarity Index Metric (SSIM): SSIM is used for evaluating the structure comparison between two patterns. [31] thought this kind of metric with the assumption that human visual processing system can perceive the pattern including its variations and distortion through extracting the structural information changes.

Based on the luminance (l), contrast (c) and structure (s) of two patterns x and y.

$$SSIM(x,y) = \left[l(x,y)^{\alpha} \cdot c(x,y)^{\beta} \cdot s(x,y)^{\gamma} \right] \quad (2)$$

When the α,β and γ equal to 1, we can get the SSIM function which I used in this paper as shown in equation (3).

$$SSIM(x,y) = \frac{(2\mu_x\mu_y + c_1)(2\sigma_{xy} + c_2)}{(\mu_x^2 + \mu_x^2 + c_1)(\sigma_x^2 + \sigma_y^2 + c_2)} \quad (3)$$

SSIM could be used for describing the the positive relation with the pattern quality between the original and reconstructed patterns. In order to show more detailed performance, we also introduce another pattern quality metric named Peak Signal to Noise Ratio (PSNR).

3) Peak Signal-to-Noise Ratio (PSNR): Given a clean pattern $\mathbf{I}_1$ and the reconstructed pattern $\mathbf{I}_2$with size $M \times N$ we can get the MSE as the same in equation (1), we can get the $PSNR$ as shown in equation 4:

$$PSNR = 10 \cdot log_{10}(\frac{MAX_I^2}{MSE}) \quad (4)$$

MAX_I^2 is the max value in whole pixel range. For instance, if we used uint8 to represent an image, MAX_I^2 should be 255 ($2^8 - 1$).

III. Results

A. One framework for multiple tasks

Our proposed model is a framework with a mixture of a biological encoding part and a DNN based decoding part as illustrated in Figure 1. The encoding part is similar to an neural pathway of the sensory systems, which receive sensory information in the format of images, sound waves, or other types of artificial sensor data represented spatial, temporal, or spatiotemporal patterns. The output of the encoder is a sequence of spikes similar to biological neurons in response to stimuli. After encoding, the encoded information will be delivered to the decoding part. Depending on practical tasks, the different decoders can be built for signal reconstruction, object recognition, semantic classification, etc. One can decode the spikes directly with spiking neural networks as decoder. Or one can also convert spikes into different format of data, for example, image pixels, to take advantage of the state-of-the-art computer vision techniques. The benefit of transcoding sensory information with neural spikes is to utilize the core concept of neuromorphic computing, e.g., energy and data efficient computing without loss of any information. Thus, our proposed framework is a unified spike transcoding system functioning as data compression, feature extraction, temporal encoding and decoding.

In this study, we put our proposed framework into the context of signal reconstruction in terms of image pixels. However, it is noted that our framework is fixable to account for other purposes, so that the exact architectures of the encoder and decoder are fixable to adapt to be other types of neural networks, or simple traditional statistical methods. To reconstruct signals, we need to upsample the encoded spikes into the remapping image space with the same size of signals, 4096 in our cases. According to the central limit theorem, these remapping images are following a Gaussian distribution. The intuition is that if one adds up all of different types of images through each detailed pixel, we would get a white-noise picture. In this sense, these remapping images are the reservoir of input information and crucial for reconstructing the final output signals to match the input signals.

As shown in Figure 1, we evaluate our model on various different datasets for different tasks.

- MNIST data [23], where there are 10 digital images, is used to demonstrate the feasibility of our model for transcoding with neural spikes.
- MNIST with random noise [24], where each digital image is embedded with a certain level of noise. Furthermore, we also used data with different levels of noise to test the model behavior, e.g. varied Gaussian noise with different noise intensities.

- MNIST with background images [24], where each digital image is embedded with a background natural image. A random patch from a white and black was used as the background. Those patches were extracted randomly from a set of pictures downloaded online.
- **CIFAR10**[32] is a RGB based dataset which consists of 50,000 training images and 10,000 test images in 10 classes, the image size is 32×32. It has natural images with complex patterns and objects which was used by the proposed DSPD to show its reconstruction ability. The same as Gaussian MNIST, we also used data with different levels of Gaussian noise to test the model denoise behavior.
- fMRI brain activity under viewing handwritten images [25], where the datasse consists of fMRI signals viewing the letters of B, R, A, I, N, S.
- Sound signals of 10 spoken letter datasets [26], where different people read 10 digits of MNIST. The dataset includes audio-image pairs which were used to build the relationship between audio waves and images.

B. Signal Reconstruction and Denoising

In order to show the capability of the proposed DSPD for signal reconstruction, we use visual images regarding to mimic the static image reconstruction as one of the most important functions in biological visual processing system. We applied DSPD on five static image datasets which are dividend into two categories: pure dataset MNIST and noisy datasets random-MNIST (with random noise), background-MNIST (with background images), rotation-MNIST (rotated digital) and rotation-background-MNIST (rotated digital with background images) as show in Fig. 3. The dataset is divided into two parts: training set (50,000 training samples) and test set (10,000 test samples) for MNIST and its variation. Different from other reconstruction models [18] [33] which only focus on image without any other noise, DSPD have strong generation ability in noisy environment caused by random (rand), background (bg), rotation (rot) and background-rotation (bg-rot).

In order to further explore the model's generalization ability in noisy environment, we divide the sizes of the training set and test set to verify that the DSPD can achieve better performance on small-size datasets than any other models. For examples, when the training samples are 90 and test samples are 10 means, we choose 90 training samples from the whole 50,000 training samples randomly and they are uniformly distributed in 0-9 ten classes.

As shown in Fig. 3, we choose standard MNIST and its four variations to show the noise immunity of DSPD, these four noisy MNIST datasets have random, background, rotation and rotation-background noise respectively. The first two rows in Fig.2 represent the qualitative evaluations showing that the DSPD have strong denoising ability when it deals with the random-MNIST and background-MNIST, the reconstructed images from random and background MNIST appear clear without noise. However, when the datasets have rotated objects, DSPD cannot reconstruct meaningful images. Presumably, because rotation is symmetrical in in all directions, that break the unity of directionality in digital images, for instances, if a handwritten image 6 is rotated more than 90 degree or even 180 degree, then it becomes some wrong types such as 9, which can not be discriminated by the model.

In order to further demonstrating that the strong rotation is more symmetrical, we used t-SNE [34] to visulize the structure of sample population represented by images after upsampling spikes (Fig. 3). From Fig. 3, one can see that when t-SNE is applied on clean MNIST images, the 0-9 ten classes could be splitted better when rot (rotation) MNIST. As shown in Fig. 3 , the encoded patterns from rotation MNIST are mixed together so that them can not be separated well. Although the patterns all look like white-noise, they are significantly different. From the encoding point of view, this could also explain the meaning about the patterns after encoding and give the reason why the reconstructed images from rotation and rotation-background MNIST look like zeros in the last two rows in Fig. 3.

Not only limited by the quality evaluations on visualization, we also make some more detailed quantitative evaluations. Table I. To show the advantage of spike transcoding,, we implement and compare our DSPD with another recent state-of-the-art method termed deep generative multi-view model (DGMM) [35]. DGMM is designed in the context of fMRI decoding, here we test it for signal reconstruction. As DGMM is designed for reconstructing small size datasets, in order to compare the reconstruction performance with DSPD, we extract a small subset from whole dataset as using 90 images for training and 10 images for rebuilding. And the MNIST and its four variations are not uniformly distributed in 50,000 training samples and 10,000 test samples, in order to avoid to the imbalanced training problem, we choose 40,000 and 8000 equally distributed training samples and 8000 test samples as the maximum experimental condition. From table I, we can see that DSPD perform better than DGMM when in small size 90 training samples and 10 test samples on MSE, SSIM and PSNR. DSPD reaches a PSNR peak at 13.11 when reconstructing from random MNIST. If the training and test samples from small size dataset (90/10) move to large size dataset (40,000/8000), these performance evaluation metrics of DSPD on random and background MNIST are better than these evaluated on 90 training and 10 test. On the whole, there is no huge performance gap on random (MSE: 0.032 SSIM: 0.52 PSNR: 14.72), background (MSE: 0.048 SSIM: 0.421 PSNR: 13.77). This is thought to be due to the increasing training samples from random and background MNIST could help train the framework and improve the decoding performance.

We then further test the model with different levels of noise. Based on the clean MNIST images, we added Gaussian noise wit increasing levels of noise by varying the parameter of σ. As shown in Fig. 2 left, we varied the degree of σ from 0 (clean) to 0.1 (strong noise). With the increasing of noise level, the images look like more fuzzy. With those noise MNIST images as input, the proposed DSPD could reconstruct the pictures as shown in Fig. 2 right. One can observe that the proposed framework could rebuild the pattern successfully and the reconstructed samples could denoise very well with different level of noise, except the strong noise ($\sigma = 0.1$),

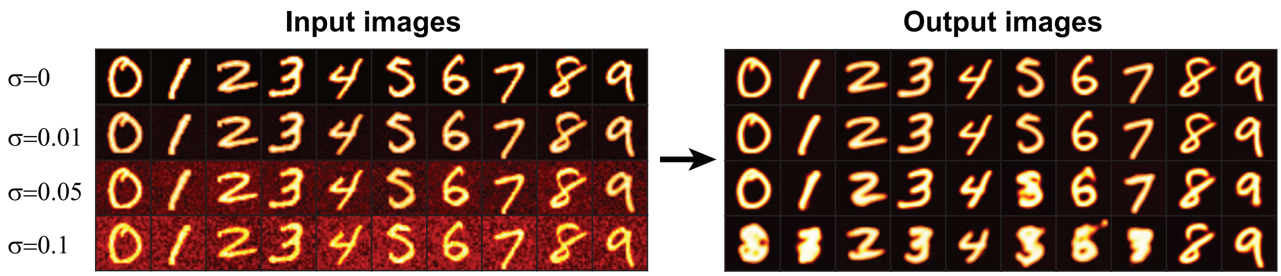

Fig. 2: Reconstructed images from noisy MNIST.

which is similar in top right corner of Fig. 3. Although the reconstructed samples with strong noise is not visually perfect as those from light noise, we can also recognize the digit shape easily.

The proposed DSPD could not only reconstruct high quality from noisy handwritten digits, but also get good reconstruction performance from noisy natural image-complexity dataset, here we adopted CIFAR10 as experimental dataset.

As shown in figure 4, with different levels of Gaussian noise (from $\sigma = 0$ to $\sigma = 0.1$), the proposed DSPD could reconstruct images from noisy CIFAR10 dataset. The proposed DSPD was trained on 50,000 images and rebuilt from 10,000 test samples. Different from MNIST digits, the proposed model could reconstruct similar quality figures with both clean noise or strong noise visually. This also means more natural images with higher complexity have strong anti-noise ability. One possible reason is that natural images with complex patterns contain more information including color, texture and shape, while digits are much more simple. So from Figure 4, the proposed DSPD show its strong anti-noise ability in real-life natural environments.

C. Reconstruction of fMRI Signals

The presented DSPD framework could not only reconstruct high-quality images and show strong noise immunity, but also perform well on object recognition from fMRI signals. We used a fMRI dataset with the simuli as handwritten letter images for testing the model. In order to show the reconstruction ability of DSPD, we also compared our DSPD with the DGMM [35]. Visually we observe that proposed DSPD can rebuild better quality patterns compared the results from DGMM.

Fig. 5 represented the reconstructed samples produced by DSPD and DGMM. Fig. 5 left are reconstructed patterns of DSPD and DGMM with 90 training samples and 10 reconstructing samples. We can observe that the proposed DSPD show more clear reconstructed samples compared to the results from DGMM. And there is a similar conclusion no matter on subjects $S1$, $S2$ and $S3$, or brain areas $V1$ and $V2$, when the training samples increased to 300 and reconstructing samples are 60 as shown in Fig. 5 right. Compared to the results from DSPD, DGMM generates more blurry reconstructed images.

Table II shows more detailed performance quantitative evaluation on fMRI Handwritten characters dataset of DSPD and DGMM. As mentioned before, this fMRI based character dataset has three subjects $S1$, $S2$ and $S3$ from $V1$ and $V2$ of human retinal systems. Here we used 300 image-fMRI pairs for training and 60 for reconstructing. As shown in table II, in subject 1 (S1), the proposed DSPD could perform bettern the DGMM on MSE, SSIM and PSNR. As for S2, DGMM could get better reconstruction performance on MSE (0.059) and PSNR (13.02) in character patterns from V2 areas, DSPD achieve the best performance on SSIM (0.45). When we observe the performance evaluation metrics located on S3, except DGMM has the best PSNR (12.508) in V1 areas, the proposed DSPD nearly behave better than DGMM on MSE and SSIM no matter in V1 and V2 areas. In short, the proposed DSPD behave better in most cases, but that is not a big difference. So, from the quality and quantitative evaluation of DSPD and DGMM, we can conclude that the proposed DSPD achieve better reconstruction performance on fMRI character datasets.

D. Decoding Sound Signal

In order to further explore the potential of our model framework, we apply it on a sound dataset with audio waveform by differnet human subjects reading 10 digits of MNIST. As shown in Fig. 6, the same as used in [26] , we choose 0-9 digits as the audio samples and standard MNIST for images (see Methods). For a single digit, the samples are collected from different human subjects reading it for audio data and writing it for MNIST image data. There are different mappings between audio digits and image digits. To induce noise and show the generalization of audio data, we designed two types of audio-image pairing dataset as shown in Fig. 6. Fig. 6 A is the dataset A, in which we choose different image samples for different audio samples in the the sample class as one image-per audio. Whileas, in dataset B, we use the same image samples to represent the same class of audio samples, which means the images in one class are the same for diffent audio samples.

For sound-image dataset A (one image-per audio) and dataset B (one image-per class), we choose a subset about 90 training samples and 10 test samples to show the reconstruction performance as shown in Fig. 7A and B. And for a further comparison, we divide the full size (4136 samples) as 4000 training samples and 136 test samples respectively, the selected reconstructed samples are presented in Fig. 7C and D. We can observe that compared to the generated from dataset B, dataset A generates more blurry images which indicate the reconstructed samples from dataset A could learn the underlying shape, structure and texture of the presented

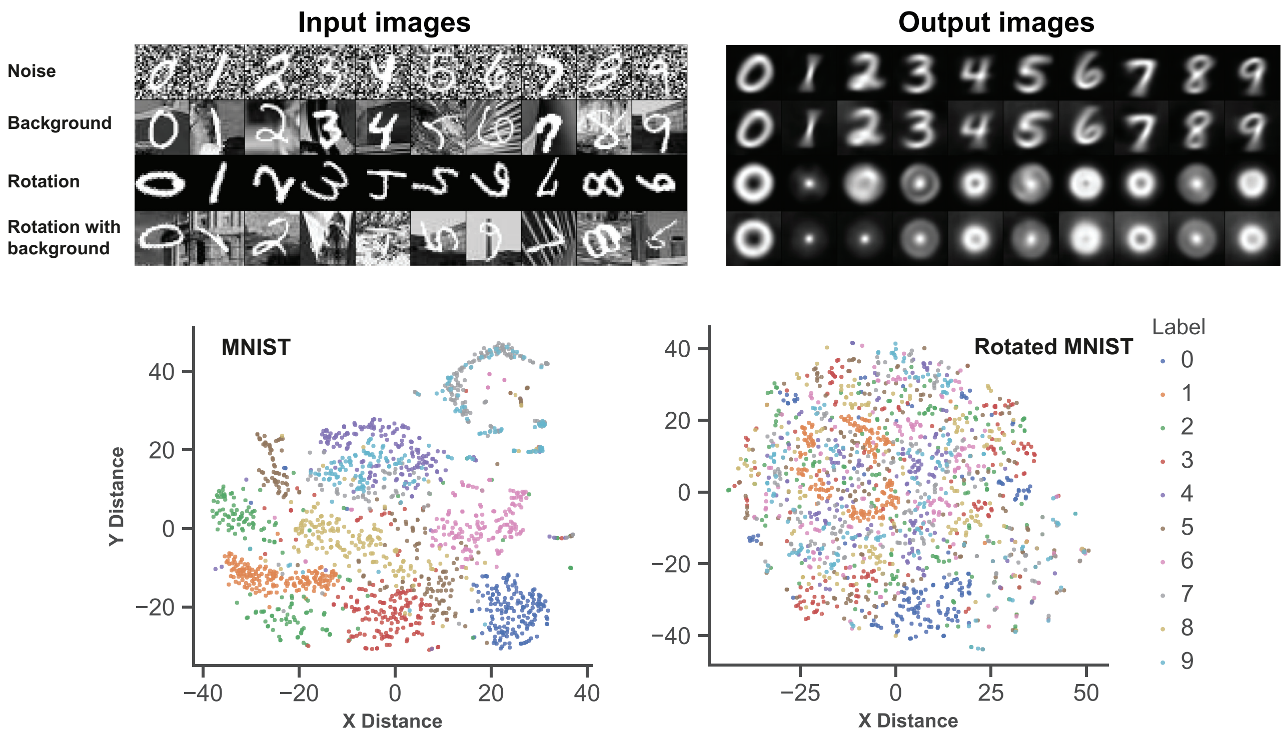

Fig. 3: Reconstructed images from different versions of MNIST. Different t-SNE visualization images between clean and rot MNIST based spatio-temporal patterns after encoding.

TABLE I: Comparison of noise immunity between DSPD and DGMM on MNIST and its variations.

	Random			Background			Rotation			Bg-rotation		
Model	MSE	SSIM	PSNR	MSE	SSIM	PSNR	MSE	SSIM	PSNR	MSE	SSIM	PSNR
DSPD (90/10)	0.049	0.15	13.11	0.056	0.381	12.90	0.072	0.417	11.67	0.087	0.290	10.99
DGMM (90/10)	0.062	0.36	12.02	0.080	0.358	11.33	0.124	0.243	9.39	0.090	0.288	10.59
DSPD (40K/8K)	0.032	0.52	14.72	0.048	0.421	13.77	0.068	0.489	11.77	0.092	0.276	10.58

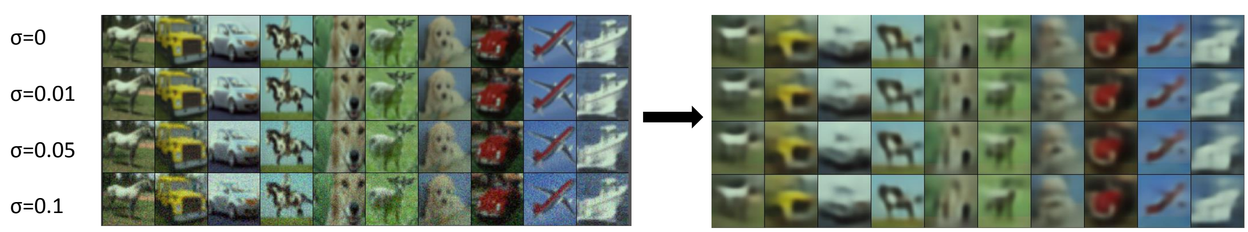

Fig. 4: Reconstructed images from noisy CIFAR10.

images, but they could not learn finer details. Although the images in dataset A are various, the proposed DSPD may learn some more different basic information such as shape, texture and structure and extract the common information among them all, the proposed model could be trained over multiple same samples of the same class, which is more easier and helpful for a network model.

IV. Discussion

In this paper, we proposed a robust cross-multimodal pattern reconstruction model named deep spike-to-pattern decoder (DSPD). This cognitive model combines neural encoding and DNN based decoding parts in a same framework, with the help of neural encoding method, this biological plausible reconstruction model can encode the outside stimuli to spatiotemporal patterns. Based on these kinds of advantages, the proposed DSPD has strong generalization ability and become robust in noisy environment. Furthermore, it is the first attempt to encode various kinds of stimuli: image, fMRI and sound in a uniform framework. We show the reconstruction performance of the presented DSPD applied on MNIST, variational MNIST, fMRI-digits datasets, fMRI-characters datasets, sound-image dataset A and dataset B is comparable to some other state-of-the art reconstruction models. We argue the encoding method and decoding structure adopted by DSPD could help to extract more important features and lead to train a more robust and efficient cognitive reconstruction model. In the future, we will adopt more types of external stimuli such as ECoG, EEG and

TABLE II: Evaluation of neural decoding performance of DGMM and proposed DSPD on fMRI character dataset with three subjects $S1$, $S2$ and $S3$ from $v1$ and $v2$ areas.

Models	Character fMRI-S1			Character fMRI-S2			Character fMRI-S3		
	MSE	SSIM	PSNR	MSE	SSIM	PSNR	MSE	SSIM	PSNR
DGMM-V1	0.068	0.212	11.87	0.060	0.266	12.79	0.069	0.27	**12.508**
DSPD-V1	0.063	0.427	**12.46**	0.067	0.43	12.38	0.064	0.46	12.35
DGMM-V2	0.071	0.210	11.83	**0.059**	0.27	**13.02**	0.079	0.29	11.95
DSPD-V2	**0.061**	**0.442**	12.44	0.063	**0.45**	12.79	**0.063**	**0.47**	12.506

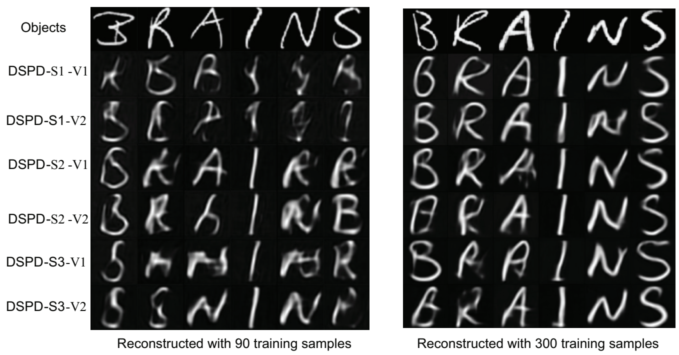

Fig. 5: Presented fMRI characters and Reconstructed Results of DSPD three subjects $S1$, $S2$ and $S3$ from the $V1$ and $V2$ areas (the left images are with 90 training samples and the right images are with 300 training samples).

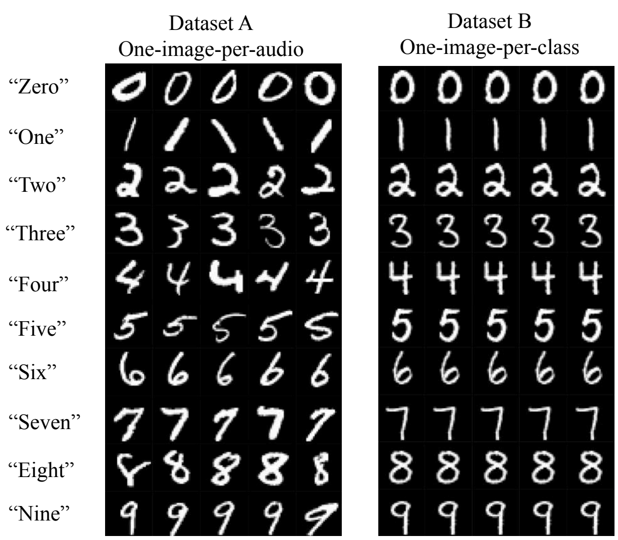

Fig. 6: Two Types of Sound Datasets. Dataset A means one image corresponds one paired audio sample, Dataset B means one image corresponds one audio class.

etc.

Because of the event driven nature of the spiking activities, it would be beneficial for implementations of neuromorphic hardware chips with aid of its structure. Furthermore, this work proposes a more biological realistic reconstruction framework which can achieve nearly real-time encoding and decoding various patterns by neural spikes. The potential showed by DSPD is promising with the hope that this cognitive model could help us how mammalian neocortex and neural circuits are performing computations in high-level visual tasks.

A. Neural Encoding and Decoding

How information is represented in the brain still remains unclear, but this leads to one of the core problems in neural processing system. However, there is strong evidence [36], [20] to believe that spike trains are an optimal way for transmission and information representation. Unlike neurons in traditional convolutional neural networks (CNNs), which communicate via real values, neurons in computational systems such as spiking neural network (SNN) communicate via spikes. Spiking based systems have been shown to be more computationally powerful than traditional artificial neural networks (ANNs), including CNNs. Moreover, these systems are event-driven, computation in synapses and neurons are triggered by incoming spikes. Driven by sparse spike trains, most synapses and neurons in neural circuits are idle for most of the time, which allows those spiking based models to run inference with low computational cost and low power. They are advantageous to deal with spatio-temporal patterns, through spike-based learning and memory mechanisms [37].

However, compared with deep CNNs, typical artificial spiking systems are surely at a great disadvantage about feature extraction because of shallow structures with few biologically based neurons. The difficulty for building a deep biological coding system lies on the complex neural dynamics, shallow layer cannot detect and capture some deeper and hidden information. [38] and [39] explored the visual system using the hierarchical simple cell and complex cell feedforward model, and showed that there is a high resemblance of the feature extraction process between the model and biological brain. Nevertheless, the previous work [38] does not model the coding flow in a biological realism way, i.e., relying on a non-biological classifier such as support vector machine. Aiming at this issue, CSNN [16] proposes a brain-inspired spiking based coding framework, which consists of a partial CNN and a SNN. CSNN is able to exploit the powerful feature extraction ability of the CNN to increase the coding performance of the computational neural system.

There still exist big challenges about constructing robust coding system which is believed to originate from the invariant representation of cross-multimodal features. In biological coding processing, the information which is received from the outside and communicate between the neurons is discrete. Before run-time, every real value of the outside image is encoded into spike trains by the feat of encoding methods, then the spikes are communicated between the corresponding neurons of the networks. The existed encoding rules can be classified into rate based coding, temporal based coding and others.

The rate based coding [40] is used to encode images into

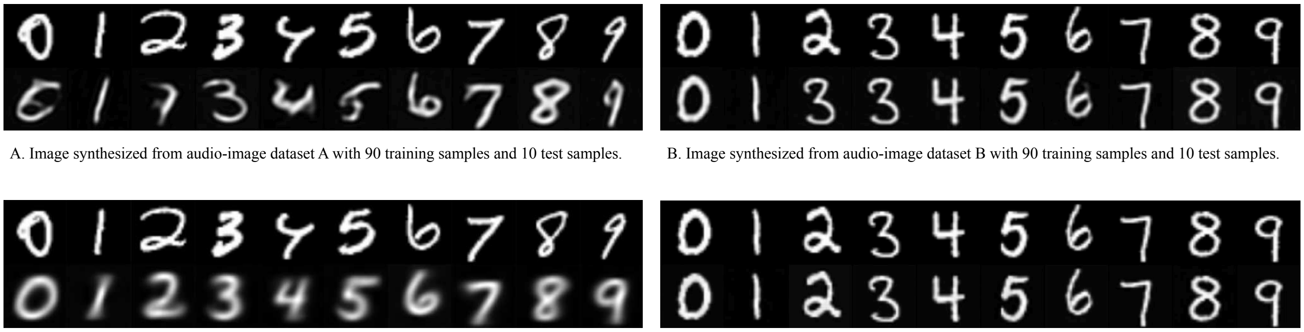

A. Image synthesized from audio-image dataset A with 90 training samples and 10 test samples.

B. Image synthesized from audio-image dataset B with 90 training samples and 10 test samples.

C. Image synthesized from audio-image dataset A with 4000 training samples and 136 test samples.

D. Image synthesized from audio-image dataset B with 4000 training samples and 136 test samples.

Fig. 7: Image synthesized from Dataset A (one image-per audio) and Dataset B (one image-per class) with small size training samples (90) and full size training samples (4000). Images in first line are the presented samples and figures in second line are reconstructed results.

dense spikes, a higher firing rate is defined as high sensory variable which can be represented as the average number of spikes counting within a temporal encoding window. The rate based coding always uses dense spikes (Poisson spike trains) to represent the neurons firing rate. To encode a real value, rate coding tends to generate many spikes, especially if the real value is large, which imposes high computational load on downstream spiking neurons. [41] proposes a novel algorithm which adopted filtered spike train as transition from original images. The sparse coding [42] clusters a relatively small subset of neurons which have nearly the same firing rate.

Although these rate based coding mechanisms are to some extent successful, the power consumption of the whole system is large. The precision of the encoded value increases with the time span of the spike train, which is roughly proportional to the number of spikes in the spike train. In addition, given the time span of the spike train, the number of spikes in the spike train is roughly proportional to the encoded value [43]. Therefore, with rate coding, many spikes have to be generated to encode a large value with high precision, which imposes a high computational load on downstream neurons. On the other hand, to generate a spike train, spikes have to be generated with different spike times. With rate coding, spike times of individual spikes are not used to convey information at all.

Furthermore, studies [44], [45] have proved that neurons in human retina firing more likely as temporal coding mechanism compared to rate based coding ways [20]. Patterns encoded from temporal coding can carry more information in spatiotemporal spikes and consume fewer computational resources than rate based coding. So based on the advantages lying in temporal encoding, this paper adopts a biological temporal encoding methods as the primary encoding layer.

Compared with the spiking neuron models such as IF, LIF, Adex, Izhikevich in SNN or Aurel Lazar's Time Encoding Machines[46], our model is not a spike-in spike-out model. We only consider the question of reconstructing visual stimuli from neuron responses, i.e. decoding is an essential part in this study. Here we propose a decoding model that reconstructs natural scenes directly from neural signals. Different from HTM[47] (hierarchical temporal memory) which focuses on time-coherent information in analysis of brain's model, we expect that our decoder will help to solve some problems on neural decoding (e.g. what characters of spikes are important for neural coding), and provide some clues on the questions of brain-machine interface, such as neural neuroprosthesis.

Some recent work[48], [49], [50] have encoded dynamic video scenes, speech and biomedical signals with DVS (Dynamic Vision Sensors) or other Neuromorphic hardware chips successful. Our proposed model is so far implemented on Ubuntu software system, in the future, we will take DVS sensors as one of the beginning of sensory information acquisition equipment and implement the DSPD model on our designed Darwin[51] Neomprphic hardware system to achieve a software-hardware integrated spiking recognition framework for artificial machine vision.

B. Multimodal Pattern Reconstruction

There has already been various studies for how to construct the visual pattern reconstruction systems. Typical visual reconstruction aim at reconstructing the original stimuli by using the neural response, for instances, rebuilding the visual scenes which the animals saw before through obtaining each pixel of those scenes from the neural signals produced by visual system, including neural spikes and fMRI activity [18] [52] [53]. [54] proposed a Bayesian canonical correlation analysis model to build a bridge between visual scenes and the corresponding brain activities, however due to the limitation of simple linear shallow framework, it cannot get some complex features. [18] [55] constructed the rebuilding systems with the aid of deep neural networks, compared to traditional simple mapping methods, these models could obtain more meaningful and complex features, thus leading to better performance. [56] combined the probabilistic inference with the generative adversarial networks and applied it into a face image - evoked brain activities, which usually cannot converge to the global optimum with the constrain of a n equilibrium between the generator and discriminator [57].

Although the aforementioned work greatly promote the research in the area of pattern reconstruction, accurately reconstructing the cross-multimodal still remains challenging from two main aspects: 1. Those models are short of more biological coding activities such as spikes encoding and decoding from with neural coding method, since the spikes generated with neural coding are the unique output neurons of retinas. 2. They only focused on one or two modals pattern reconstruction tasks such as fMRI and images, cross-multimodal pattern rebuilding is necessary and pivotal for understanding how neural representation in biological neural system. In order to address these limitations, this paper proposed a cross multi-modal pattern reconstruction with hierarchical structures from spiking activities, named deep spike-to-pattern decoder (DSPD). Recent advances in experimental techniques enables us to record neural signals from multiple brain areas simultaneously [58]. Thus, our proposed decoding approach make it possible to decoding of multimodal information from neural signals of multiple brain areas with one single decoding framework. We expect that the method presented here will advance the methodology of analyzing neural spikes, as well as the applicability of neuromorphic computing.

References

[1] M. Jazayeri and J. A. Movshon, "Optimal representation of sensory information by neural populations," *Nature neuroscience*, vol. 9, no. 5, pp. 690–696, 2006.

[2] Z. Yu, J. K. Liu, S. Jia, Y. Zhang, Y. Zheng, Y. Tian, and T. Huang, "Toward the next generation of retinal neuroprosthesis: Visual computation with spikes," *Engineering*, vol. 6, no. 4, pp. 449–461, apr 2020.

[3] M. C.-K. Wu, S. V. David, and J. L. Gallant, "Complete functional characterization of sensory neurons by system identification," *Annu. Rev. Neurosci.*, vol. 29, pp. 477–505, 2006.

[4] E. P. Simoncelli and B. A. Olshausen, "Natural image statistics and neural representation," *Annual review of neuroscience*, vol. 24, no. 1, pp. 1193–1216, 2001.

[5] J. K. Liu and D. V. Buonomano, "Embedding multiple trajectories in simulated recurrent neural networks in a self-organizing manner," *Journal of Neuroscience*, vol. 29, no. 42, pp. 13 172–81, 2009.

[6] H. Tang, K. C. Tan, and Z. Yi, *Neural networks: computational models and applications*. Springer Science & Business Media, 2007, vol. 53.

[7] Q. Xu, J. Peng, J. Shen, H. Tang, and G. Pan, "Deep CovDenseSNN: A hierarchical event-driven dynamic framework with spiking neurons in noisy environment," *Neural Networks*, vol. 121, pp. 512–519, 2020.

[8] Y. LeCun, Y. Bengio, and G. Hinton, "Deep learning," *nature*, vol. 521, no. 7553, pp. 436–444, 2015.

[9] S. Nishimoto, A. T. Vu, T. Naselaris, Y. Benjamini, B. Yu, and J. L. Gallant, "Reconstructing visual experiences from brain activity evoked by natural movies," *Current Biology*, vol. 21, no. 19, pp. 1641–1646, 2011.

[10] T. Horikawa, M. Tamaki, Y. Miyawaki, and Y. Kamitani, "Neural decoding of visual imagery during sleep," *Science*, vol. 340, no. 6132, pp. 639–642, 2013.

[11] K. N. Kay, T. Naselaris, R. J. Prenger, and J. L. Gallant, "Identifying natural images from human brain activity," *Nature*, vol. 452, no. 7185, pp. 352–355, 2008.

[12] T. Naselaris, R. J. Prenger, K. N. Kay, M. Oliver, and J. L. Gallant, "Bayesian reconstruction of natural images from human brain activity," *Neuron*, vol. 63, no. 6, pp. 902–915, 2009.

[13] D. L. K. Yamins and J. J. Dicarlo, "Using goal-driven deep learning models to understand sensory cortex," *Nature Neuroscience*, vol. 19, no. 3, p. 356, 2016.

[14] Q. Yan, Y. Zheng, S. Jia, Y. Zhang, Z. Yu, F. Chen, Y. Tian, T. Huang, and J. K. Liu, "Revealing fine structures of the retinal receptive field by deep-learning networks," *IEEE Transactions on Cybernetics*, pp. 1–12, 2020.

[15] C. F. Cadieu, H. Hong, D. L. Yamins, N. Pinto, D. Ardila, E. A. Solomon, N. J. Majaj, and J. J. DiCarlo, "Deep neural networks rival the representation of primate IT cortex for core visual object recognition," *PLoS Comput Biol*, vol. 10, no. 12, p. e1003963, 2014.

[16] Q. Xu, Y. Qi, H. Yu, J. Shen, H. Tang, and G. Pan, "CSNN: An Augmented Spiking based Framework with Perceptron-Inception." in *IJCAI*, 2018, pp. 1646–1652.

[17] V. Botella-Soler, S. Deny, G. Martius, O. Marre, and G. Tkačik, "Nonlinear decoding of a complex movie from the mammalian retina," *PLoS Computational Biology*, vol. 14, no. 5, p. e1006057, 2018.

[18] Y. Zhang, S. Jia, Y. Zheng, Z. Yu, Y. Tian, S. Ma, T. Huang, and J. K. Liu, "Reconstruction of natural visual scenes from neural spikes with deep neural networks," *Neural Networks*, vol. 125, pp. 19–30, 2020.

[19] J. K. Liu, H. M. Schreyer, A. Onken, F. Rozenblit, M. H. Khani, V. Krishnamoorthy, S. Panzeri, and T. Gollisch, "Inference of neuronal functional circuitry with spike-triggered non-negative matrix factorization," *Nature communications*, vol. 8, no. 1, pp. 1–14, 2017.

[20] A. Onken, J. K. Liu, P. C. R. Karunasekara, I. Delis, T. Gollisch, and S. Panzeri, "Using matrix and tensor factorizations for the single-trial analysis of population spike trains," *PLoS Computational Biology*, vol. 12, no. 11, p. e1005189, nov 2016.

[21] R. L. Jenison, J. W. Schnupp, R. A. Reale, and J. F. Brugge, "Auditory space-time receptive field dynamics revealed by spherical white-noise analysis," *Journal of Neuroscience*, vol. 21, no. 12, pp. 4408–4415, 2001.

[22] W. J. Speechley, J. L. Hogsden, and H. C. Dringenberg, "Continuous white noise exposure during and after auditory critical period differentially alters bidirectional thalamocortical plasticity in rat auditory cortex in vivo," *European Journal of Neuroscience*, vol. 26, no. 9, pp. 2576–2584, 2007.

[23] Y. LeCun, C. Cortes, and C. J. Burges, "The MNIST database of handwritten digits, 1998," *URL http://yann. lecun. com/exdb/mnist*, vol. 10, p. 34, 1998.

[24] H. Larochelle, D. Erhan, A. Courville, J. Bergstra, and Y. Bengio, "An empirical evaluation of deep architectures on problems with many factors of variation," in *Proceedings of the 24th international conference on Machine learning*, 2007, pp. 473–480.

[25] S. Schoenmakers, M. Barth, T. Heskes, and M. Van Gerven, "Linear reconstruction of perceived images from human brain activity," *NeuroImage*, vol. 83, pp. 951–961, 2013.

[26] D. Roy, P. Panda, and K. Roy, "Synthesizing Images From Spatio-Temporal Representations Using Spike-Based Backpropagation," *Frontiers in neuroscience*, vol. 13, p. 621, 2019.

[27] M. Liberman, R. Amsler, K. Church, E. Fox, C. Hafner, J. Klavans, M. Marcus, B. Mercer, J. Pedersen, P. Roossin *et al.*, "Ti 46-word," *Philadelphia (Pennsylvania): Linguistic Data Consortium*, 1993.

[28] M. Slaney, "Auditory toolbox," *Interval Research Corporation, Tech. Rep*, vol. 10, no. 1998, 1998.

[29] M. Abadi, P. Barham, J. Chen, Z. Chen, A. Davis, J. Dean, M. Devin, S. Ghemawat, G. Irving, M. Isard *et al.*, "Tensorflow: A system for large-scale machine learning," in *12th {USENIX} Symposium on Operating Systems Design and Implementation ({OSDI} 16)*, 2016, pp. 265–283.

[30] A. Gulli and S. Pal, *Deep learning with Keras*. Packt Publishing Ltd, 2017.

[31] D. Brunet, E. R. Vrscay, and Z. Wang, "On the mathematical properties of the structural similarity index," *IEEE Transactions on Image Processing*, vol. 21, no. 4, pp. 1488–1499, 2011.

[32] A. Krizhevsky and G. Hinton, "Learning multiple layers of features from tiny images," *Handbook of Systemic Autoimmune Diseases*, vol. 1, no. 4, 2009.

[33] Y.-T. Lin and G. D. Finlayson, "Physically Plausible Spectral Reconstruction from RGB Images," *arXiv preprint arXiv:2001.00558*, 2020.

[34] L. v. d. Maaten and G. Hinton, "Visualizing data using t-SNE," *Journal of machine learning research*, vol. 9, no. Nov, pp. 2579–2605, 2008.

[35] C. Du, C. Du, L. Huang, and H. He, "Reconstructing perceived images from human brain activities with bayesian deep multiview learning," *IEEE transactions on neural networks and learning systems*, vol. 30, no. 8, pp. 2310–2323, 2018.

[36] C. P. Hung, G. Kreiman, T. Poggio, and J. J. Dicarlo, "Fast Readout of Object Identity from Macaque Inferior Temporal Cortex," *Science*, vol. 310, no. 5749, pp. 863–866, 2005.

[37] J. Hu, H. Tang, K. C. Tan, and H. Li, "How the Brain Formulates Memory: A Spatio-Temporal Model Research Frontier," *IEEE Computational Intelligence Magazine*, vol. 11, no. 2, pp. 56–68, 2016.

[38] T. Serre, A. Oliva, and T. Poggio, "A feedforward architecture accounts for rapid categorization." *Proceedings of the National Academy of Sciences of the United States of America*, vol. 104, no. 15, pp. 6424–6429, 2007.

[39] T. Serre and T. Poggio, "A Neuromorphic Approach to Computer Vision," *Communications of the Acm*, vol. 53, no. 10, pp. 54–61, 2010.

[40] O. Peter, N. Daniel, S. C. Liu, D. Tobi, and P. Michael, "Real-time classification and sensor fusion with a spiking deep belief network," *Frontiers in Neuroscience*, vol. 7, p. 178, 2013.

[41] P. Merolla, J. Arthur, F. Akopyan, N. Imam, R. Manohar, and D. S. Modha, "A digital neurosynaptic core using embedded crossbar memory with 45pj per spike in 45nm," in *Custom Integrated Circuits Conference*, 2011, pp. 1–4.

[42] L. Perrinet, M. Samuelides, and S. Thorpe, "Sparse spike coding in an asynchronous feed-forward multi-layer neural network using matching pursuit," *Neurocomputing*, vol. 57, pp. 125–134, 2004.

[43] M. Wang, X. Liao, R. Li, S. Liang, R. Ding, J. Li, J. Zhang, W. He, K. Liu, J. Pan, Z. Zhao, T. Li, K. Zhang, X. Li, J. Lyu, Z. Zhou, Z. Varga, Y. Mi, Y. Zhou, J. Yan, S. Zeng, J. K. Liu, A. Konnerth, I. Nelken, H. Jia, and X. Chen, "Single-neuron representation of learned complex sounds in the auditory cortex," *Nature Communications*, vol. 11, no. 1, aug 2020.

[44] M. J. Berry and M. Meister, "Refractoriness and neural precision." *Journal of Neuroscience*, vol. 18, no. 6, p. 2200, 1998.

[45] V. J. Uzzell and E. J. Chichilnisky, "Precision of spike trains in primate retinal ganglion cells." *Journal of Neurophysiology*, vol. 92, no. 2, pp. 780–9, 2004.

[46] A. A. Lazar and Y. Zhou, "Reconstructing natural visual scenes from spike times," *Proceedings of the IEEE*, vol. 102, no. 10, pp. 1500–1519, 2014.

[47] J. Hawkins and D. George, "Hierarchical temporal memory," *Alphascript Publishing*, vol. suppl, no. 5, pp. 1 – 10, 2011.

[48] M. Yang, S. C. Liu, and T. Delbruck, "Comparison of spike encoding schemes in asynchronous vision sensors: Modeling and design," in *IEEE International Symposium on Circuits & Systems*, 2014.

[49] Minhao, Yang, Shih-Chii, Liu, Tobi, and Delbruck, "Analysis of encoding degradation in spiking sensors due to spike delay variation," *IEEE Transactions on Circuits & Systems I Regular Papers*, 2017.

[50] F. Corradi, C. Eliasmith, and G. Indiveri, "Mapping arbitrary mathematical functions and dynamical systems to neuromorphic vlsi circuits for spike-based neural computation," in *IEEE International Symposium on Circuits & Systems*, 2014.

[51] D. Ma, J. Shen, Z. Gu, M. Zhang, X. Zhu, X. Xu, Q. Xu, Y. Shen, and G. Pan, "Darwin: A neuromorphic hardware co-processor based on spiking neural networks," *Journal of Systems Architecture*, vol. 77, pp. 43–51, 2017.

[52] J.-D. Haynes and G. Rees, "Predicting the orientation of invisible stimuli from activity in human primary visual cortex," *Nature neuroscience*, vol. 8, no. 5, pp. 686–691, 2005.

[53] E. Chong, A. M. Familiar, and W. M. Shim, "Reconstructing representations of dynamic visual objects in early visual cortex," *Proceedings of the National Academy of Sciences*, vol. 113, no. 5, pp. 1453–1458, 2016.

[54] Y. Fujiwara, Y. Miyawaki, and Y. Kamitani, "Modular encoding and decoding models derived from bayesian canonical correlation analysis," *Neural computation*, vol. 25, no. 4, pp. 979–1005, 2013.

[55] Y. Rivenson, Y. Zhang, H. Günaydın, D. Teng, and A. Ozcan, "Phase recovery and holographic image reconstruction using deep learning in neural networks," *Light: Science & Applications*, vol. 7, no. 2, pp. 17 141–17 141, 2018.

[56] Y. Güçlütürk, U. Güçlü, K. Seeliger, S. Bosch, R. van Lier, and M. A. van Gerven, in *Advances in Neural Information Processing Systems*, 2017, pp. 4246–4257.

[57] S. Martin Arjovsky and L. Bottou, "Wasserstein Generative Adversarial Networks," in *Proceedings of the 34 th International Conference on Machine Learning, Sydney, Australia*, 2017.

[58] M. Yang, Z. Zhou, J. Zhang, S. Jia, T. Li, J. Guan, X. Liao, B. Leng, J. Lyu, K. Zhang, M. Li, Y. Gong, Z. Zhu, J. Yan, Y. Zhou, J. K. Liu, Z. Varga, A. Konnerth, Y. Tang, J. Gao, X. Chen, and H. Jia, "MATRIEX imaging: multiarea two-photon real-time in vivo explorer," *Light: Science & Applications*, vol. 8, no. 1, nov 2019.